AIAA JOURNAL
Vol. 46, No. 7, July 2008

Novel Kevlar-Walled Wind Tunnel for Aeroacoustic Testing of a Landing Gear

Marcel C. Remillieux,* Hugo E. Camargo,† Patricio A. Ravetta,‡
Ricardo A. Burdisso,§ and Wing F. Ng¶
Virginia Polytechnic Institute and State University,
Blacksburg, Virginia 24061

DOI: 10.2514/1.33082

Experiments were conducted on a high-fidelity, model-scale, main landing gear in the Virginia Polytechnic Institute and State University Stability Wind Tunnel. This wind tunnel was recently upgraded to an anechoic facility, which allowed aeroacoustic measurements to be carried out in the far field and in an environment with significantly less reflections. The model was a very faithful replica of the full-scale landing gear, designed to address the issues associated with low-fidelity models. A 63-element microphone phased array was used to locate the noise-source components of the landing gear from different streamwise positions, both in the near and far fields. The same landing-gear model was previously tested in the original hard-walled configuration of the tunnel with the same phased array mounted on the wall of the test section (i.e., near-field position). The new anechoic configuration of the Virginia Polytechnic Institute and State University wind tunnel offered a unique opportunity to directly compare data collected in hard-walled and semi-anechoic test sections, using the same landing-gear model and phased-array instrumentation. Through these tests, some of the limitations associated with testing in hard-walled wind tunnels were addressed.

Nomenclature

C_j	=	components of the steering vector
d	=	distance from the array to the model
f	=	frequency
$f_{\text{full-scale}}$	=	full-scale frequency
f_{measured}	=	measured frequency
k	=	wave number
M	=	flow Mach number
r_j	=	distance traveled by an acoustic ray from the grid point with coordinates x_n to array microphone j
R_j	=	distance between the grid point with coordinates x_n and array microphone j
x_n	=	coordinates of the grid point to which the array is being steered
λ	=	wavelength

I. Introduction

THE expected growth in air traffic and the more stringent noise regulations imposed by the aviation authorities are forcing the aircraft industry to develop increasingly quieter aircraft. The engines and the airframe constitute the main components of the overall aircraft noise. With the introduction of high-bypass-ratio turbofan engines in the 1970s, significant engine noise reduction could be achieved. As a result, the relative noise contribution of the airframe to the overall aircraft noise has increased. This is particularly true on approach to landing, when the high-lift devices are extended and the landing gears are deployed. In such conditions, airframe and engine noise levels have become comparable.

Over the last two decades, a considerable amount of work has been devoted to locating and controlling the specific components of the airframe noise. Flight tests provide accurate noise measurements but are mainly used for noise-certification purposes, due to their prohibitive cost. Therefore, most of the recent aeroacoustic studies have been conducted in wind-tunnel facilities. Typically, open-jet and hard-walled wind tunnels are the two types of facilities encountered. Early research on airframe noise was exclusively conducted in open-jet wind tunnels because these facilities usually allow noise measurements to be carried out in the far field and in an anechoic environment. The advent of microphone phased arrays in the early 1990s has rendered possible, and even common, the ability to collect acoustic data in hard-walled wind tunnels. Phased-array postprocessing techniques allow airframe noise components to be located and quantified in the near field of a model, regardless of the background noise and reflections. However, the validity of phased-array outputs obtained in such conditions may be questioned and needs to be assessed. Furthermore, in a hard-walled wind tunnel, a microphone phased array has to be flush-mounted or recessed behind a wall of the test section. As a result, noise measurements usually have to be performed straight in front of the model to avoid distortion effects. In these conditions, it is difficult to study the directivity of a model.

To address some of the limitations of conducting aeroacoustic studies in hard-walled wind tunnels, noise measurements on a model-scale landing gear were performed. In addition to this specific application, landing gears are of particular importance themselves because they were shown to be the major airframe noise-source components in the case of modern commercial aircraft [1]. A landing gear is a very complex structure, primarily designed to support the load of a landing aircraft. To ease inspection and maintenance, the aerodynamic design is not refined. As a result, many components that are arranged in a very complex manner are exposed to the flow, which allows for noise generation through the mechanisms of steady and unsteady wake flow, turbulent flow, and vortex instability and deformation [2]. Typically, a landing gear consists of a main strut, braces that allow the gear to be retracted inside the aircraft, a varying

Presented as Paper 3453 at the 13th AIAA/CEAS Aeroacoustics Conference, Rome, 21–23 May 2007; received 26 June 2007; revision received 21 February 2008; accepted for publication 23 February 2008.

*Graduate Research Assistant, Mechanical Engineering Department, Mail Code 0238. Student Member AIAA.

†Graduate Research Assistant, Mechanical Engineering Department, Mail Code 0238. Student Member AIAA.

‡Ph.D. Alumnus, Mechanical Engineering Department, Mail Code 0238. Member AIAA.

§Professor, Mechanical Engineering Department, Mail Code 0238. Member AIAA.

¶Chris Kraft Endowed Professor, Mechanical Engineering Department, Mail Code 0238. Associate Fellow AIAA.

number of wheels (usually ranging from two to six for main landing gears), and smaller components. The small components include the brake braces, hydraulic hoses, electric wires, screw holes, and small irregularities. The smaller the characteristic dimension of a landing-gear component, the larger the frequency of the radiated noise. Dobrzynski and Buchholz [3] showed that landing-gear aerodynamic noise is essentially broadband. Noise levels in one-third octave bands are almost constant, from low frequencies up to a few thousands of hertz. In terms of levels, in low Mach number flows with rigid bodies, the noise is often scaled by the sixth power of the flow velocity [4]. Guo et al. [5] showed that this is only true for low- and midfrequency noise, which is typical of dipolelike sources. High-frequency noise is better scaled by the seventh power law, which is typical of noise generated by turbulent flow.

A comprehensive aeroacoustic study of a high-fidelity, 26%-scale, Boeing 777 main landing gear was carried out in the Virginia Polytechnic Institute and State University (VT) hard-walled wind tunnel [6,7]. This study allowed the noise-source components of the landing gear to be located and ranked from various positions of the phased array (straight underneath the wheels, on the door side, and on the brace side). Recently, the VT Stability Wind Tunnel was upgraded to an anechoic facility. The renovation of the facility was based on a novel concept that renders the test section aerodynamically closed and acoustically open [8]. The facility includes a Kevlar-walled test section. The Kevlar walls are nearly transparent to sound, eliminate the need for a jet catcher, and significantly reduce aerodynamic interference. This new concept resulted in a facility that achieves better aerodynamic performance than a free-jet facility, while maintaining comparable acoustic performance. The facility is also unique in that the anechoic system can be removed and replaced by the hard-walled test section to fully restore the aerodynamic capabilities of the facility. In addition, the anechoic system may be easily adjusted from a full- to a semi-anechoic configuration. Experiments were conducted to examine the performance of this new wind tunnel under a range of conditions, including tests on a NACA 0012 airfoil and comparison of the results with past experiments [9]. This new configuration of the VT wind tunnel allows noise measurements to be carried out in the far field and in an environment with significantly less reflections. A unique opportunity was given to directly compare acoustic data collected in hard-walled and semi-anechoic test sections using the same facility, landing-gear model, and measurement systems. The validity of performing phased-array measurements in hard-walled wind tunnels could thus be assessed. The tests also allowed the new test-section design concept to be validated.

This paper is organized as follows. Section II describes the experimental setup for measurement of the landing-gear noise, which includes the model-scale gear, the microphone phased array, the wind-tunnel facility, and the tests configurations. Section III reports the experimental results. First, phased-array data collected in hard-walled and semi-anechoic test sections are compared to evaluate the effects of the acoustic environment on the phased-array measurement. Then the validity of taking phased-array measurements in the near field is discussed by comparing acoustic data collected in the near and far fields in the semi-anechoic configuration of the wind tunnel. Last, results from two different far-field streamwise positions are compared. Conclusions are given in Sec. IV.

II. Experimental Setup

A. Landing-Gear Model

Experiments were conducted on a high-fidelity 26%-scale model of the Boeing 777 main landing gear. This model, provided by NASA, was designed to address the issues associated with low-fidelity models. Figure 1 shows the Boeing 777 landing-gear model. The key gear components are also identified in this figure. The major parts constituting the primary structural framework were made of steel and aluminum. Using stereolithography, most of the full-scale details were reproduced with accuracy down to 0.12 in. in full scale. The details include wheel hubs, brakes cylinders, hydraulic valves,

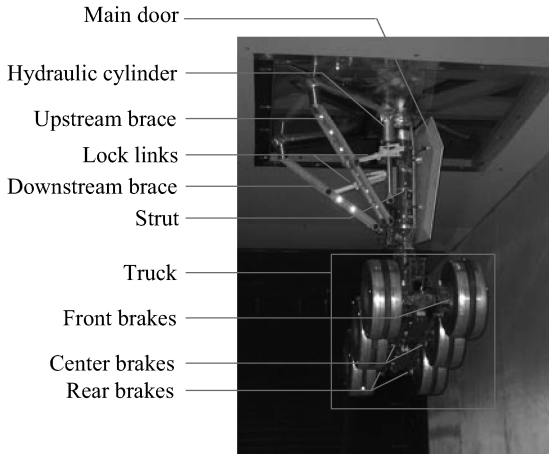

Fig. 1 The 26%-scale, high-fidelity, Boeing 777 main landing-gear model.

and so forth. Other significant details that are not present in the low-fidelity model are the hydraulic lines and cables that were reproduced using electrical wires. Although the small-scale model is a very faithful representation of the full-scale gear, several details were omitted. For instance, the small door mounted on the top of the main door in the full-scale landing gear is not present in the 26%-scale model. Also, wheel hubs in the model do not allow air to pass through. The wing cavity, in which the landing gear is stored in the cruise configuration of the aircraft, is not modeled in this study.

B. Microphone Phased Array and Postprocessing

The acoustic data acquisition was carried out with the 63-element microphone phased array depicted in Fig. 2a. This array was designed for VT by The Boeing Company. The microphones of the phased array (Panasonic WM-60AY Electret microphones) were patterned in a multi-arm spiral manner, as depicted in Fig. 2b. The microphones were found to be reliable only up to about 20 kHz; that is, the microphone signal rolled off steeply around 20 kHz. An aluminum plate was used to position the microphones accurately. Tapped holes in the plate, at the microphone locations, allowed the custom-made microphone adaptors to be bolted in the plate so that the microphones were mounted flush with the plate surface.

The 63 microphone signals were sampled simultaneously at 51,200 samples per second in 25 separate blocks of 16,384 samples each. Time-domain data were processed using a frequency-domain, phased-array, beam-forming code developed at VT that accounts for the flow in the test section and the sound refraction through the flow velocity discontinuity between the test section and the anechoic chamber. As shown in Fig. 3, when sound propagates from source points to a microphone in the array, part of the acoustic path is in the flow and part is outside of it. If conventional beam-forming is used, an apparent source will be located downstream of the actual source. In the revised beam-forming algorithm used here, the components of the steering vector were given by the solution of the convected-wave equation:

$$C_j(\mathbf{x}_n) = \frac{e^{-ikr_j}}{4\pi R_j} \tag{1}$$

where $\mathbf{x}_n$ are the coordinates of the grid point to which the array is being steered, k is the wave number, R_j is the distance between the grid point with coordinates $\mathbf{x}_n$ and microphone j, and r_j is the distance traveled by the ray to microphone j. The ray path is computed by following the numerical ray-tracing technique developed by Candel [10] and summarized by Pierce [11].

Acoustic data were processed from 2 to 20 kHz in one-twelfth-octave bands. The spatial resolution of the array will be given in terms of the beam width (BW): the region of the beam-forming map within 3 dB of the peak level. Thus, for a plane located at 36 in. from the array, the beam width was found to be $\mathrm{BW}_{36} = 2.22\lambda$, where λ is

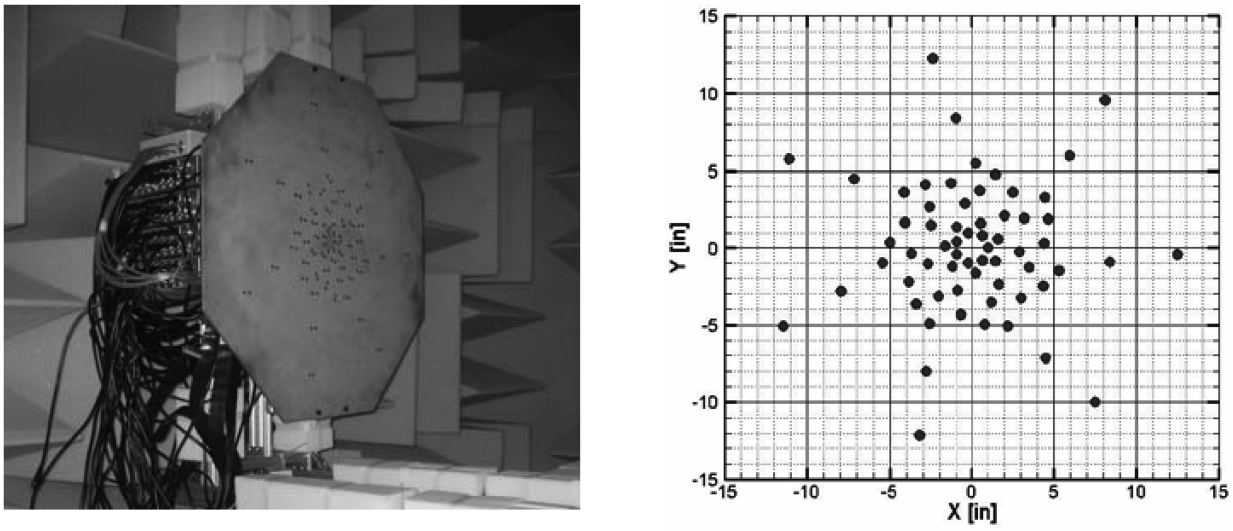

a) b)

Fig. 2 The 63-element microphone phased array used for noise-source location a) photograph and b) schematic of the array pattern.

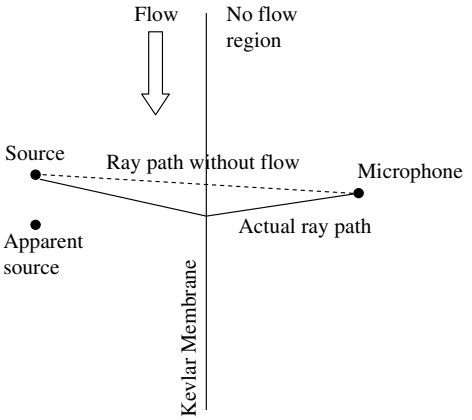

Fig. 3 Sound-wave propagation through a flow velocity discontinuity using ray acoustics.

the sound-wave length. The signal-to-noise ratio (SNR) as a function of frequency for a plane at 36 in. from the array is depicted in Fig. 4. The lowest SNR is about 8.7 dB at 19 kHz.

In all cases, the postprocessing was carried out over the same scanning grid, which had dimensions of $70 \times 56 \times 39$ in., contained 323,031 points, and encompassed the entire landing gear.

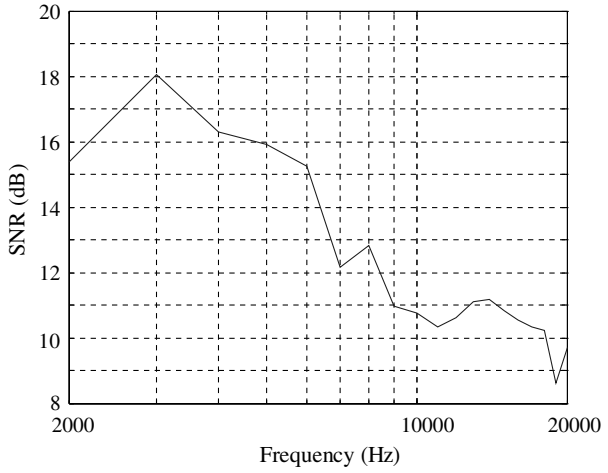

Fig. 4 Signal-to-noise ratio of the array as a function of frequency for a plane at 36 in. from the array.

The array was calibrated for phase to account for phase mismatch in the microphone signals and for errors in microphone positions. The array was also calibrated for amplitude. Tests were conducted in the VT semi-anechoic wind tunnel to determine the sensitivity of the array, to account for the presence of the Kevlar window and the dissipation effects due to the flow.

Note that the array of microphones was mounted on a finite plate. For this reason, the signals recorded by the microphones located close to the edge of this plate may be subjected to edge effects such as diffraction and scattering. For the calibration of the phased array, a monopolelike source was installed at various locations in the test section and its noise levels were measured both with a single microphone and the phased array. Levels obtained with the single microphone and the integrated spectra are virtually the same [12]. Therefore, the effects from the array mounting on the results are likely small and were not accounted for in this study.

C. Wind-Tunnel Facility

The landing gear was mounted in the VT Stability Wind Tunnel. Originally, it was a NACA facility located at Langley Field in Virginia, designed to provide a very-low-turbulence-level flow for dynamic stability measurements. Figure 5a is a schematic description of the original VT hard-walled wind tunnel. The facility is a continuous-single-return subsonic wind tunnel. The tunnel is powered by a 0.45-MW variable-speed dc motor driving a 14.1-ft propeller at up to 600 rpm. Although the tunnel forms a closed loop, it has an air-exchange tower open to the atmosphere to allow for temperature stabilization. The air-exchange tower is located downstream of the fan and motor assemblies. Downstream of the tower, the flow is directed into an 18×18 ft settling chamber containing seven turbulence-reducing screens, each with an open-area ratio of 0.6 and separated by 5.9 in. The test section is 24 ft long with a constant square cross section of 6 ft. The original hard-walled test section is shown in Fig. 5b. The flow passing through the test section undergoes a 9:1 area contraction. The test section is enclosed in an airtight control room so that the pressure in the control room equates the pressure in the test section via a window located downstream of the test section. The problem of air leakage into the test section flow is thus minimized. At the downstream end of the test section, flow passes into a 3-deg diffuser. The four corners in the flow path (two between the air-exchange tower and settling chamber and two between the diffuser and fan) are equipped with diagonal arrays of shaped turning vanes.

Since its installation at VT, the wind tunnel has undergone a series of modifications such as the renovation of the fan and a reinsulation of the motor windings, resulting in the increase of the overall tunnel

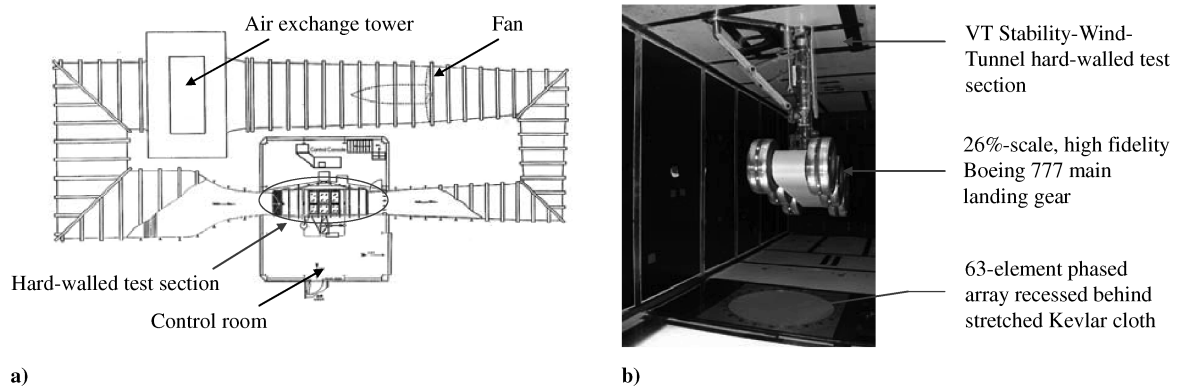

Fig. 5 VT Stability Wind Tunnel in its original hard-walled configuration: a) plan-view schematic of the tunnel circuit and b) photograph of the landing gear installed in the hard-walled test section.

efficiency. Although the Stability Wind Tunnel was shown to have very good flow quality and was used for aeroacoustic measurements in the past, it was not primarily built as a quiet facility.

Recently, as part of a project to render the Stability Wind Tunnel suitable for aeroacoustic measurements, the hard-walled test section was removed and replaced by an anechoic system. Figure 6a is a CAD drawing of the test section in its semi-anechoic configuration. Note that the test section may also be used in a fully anechoic configuration. The semi-anechoic configuration was necessary in this case to mount the landing gear in the test section. The bottom and the top of the test section (Figs. 6a and 6b) were fitted with acoustic treatment. Stretched Kevlar membranes glued on perforated metal sheets separated the flow area from the acoustic treatment. A hard wall with a sealable window was mounted on one side to allow the model to be mounted sideways in the test section. An anechoic chamber (Fig. 6c) was mounted on the side opposite to the model, and the corresponding hard-wall was replaced by a Kevlar window (Figs. 6b and 6c). The lower limiting frequency of the absorptive treatment in the test section and in the anechoic chamber was found to be 250 Hz. Because of the presence of the landing gear in the test section, the center of the Kevlar window was deflected toward the anechoic chamber, which potentially produced a change in local flow speed around the landing gear. However, the amplitude of the deflection was relatively small (e.g., estimated to be less than an inch at $M = 0.17$). Such deflection caused a change in flow speed of about 1%, which is insignificant.

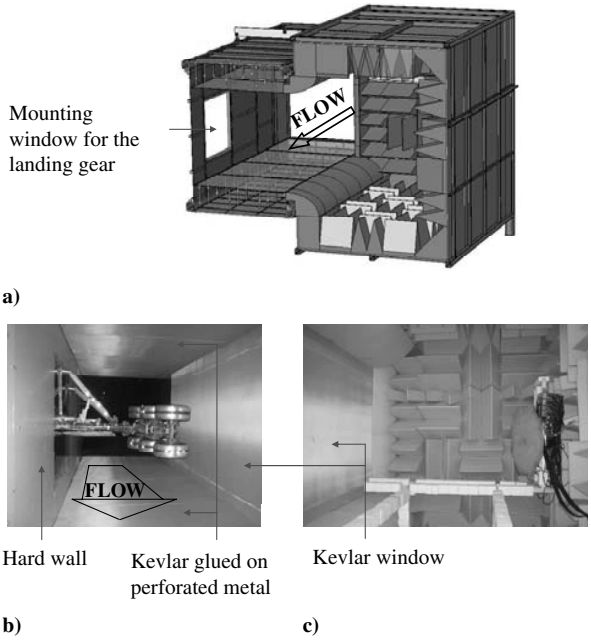

Fig. 6 Semi-anechoic system replacing the hard-walled test section: a) 3D-CAD drawing of the system, b) 26%-scale landing gear mounted in the semi-anechoic test section, and c) 63-element microphone phased array installed in the anechoic chamber.

Stretched Kevlar membranes were first used in aeroacoustic measurements by Jaeger et al. [13] as an answer to flow-induced noise. Relevant properties of Kevlar for aeroacoustic measurements were as follows: 1) very high strength and durability that makes it tolerate flow-induced fatigue very well; 2) when stretched, it appears as a hard surface to the flow; and 3) very low acoustic impedance up to high frequencies. Depending on the type of fabrics used, the acoustic attenuation may vary. In this application, 1.7-oz/in.^{2} plain-weave Kevlar 120 was chosen. Jaeger et al. [13] found that the insertion loss varied from nearly 0 at low frequencies to about 2 dB at 25 kHz.

Although the flow was contained in the test section, the sound generated by the model in the test section was allowed to propagate through the Kevlar to the anechoic chamber in which the phased array was located. In this sense, this hybrid facility is similar to an open-jet wind tunnel from an acoustic point of view and similar to a hard-walled wind tunnel from the fluid point of view.

D. Testing Configurations

Figures 7a and 7b show schematics of the experimental setup for phased-array measurements of the landing-gear noise in hard-walled and semi-anechoic test sections, respectively. In the hard-walled configuration of the test section (Fig. 7a), the phased array was located in the near field, straight under the landing gear. The array was recessed 2.75 in. behind a Kevlar membrane. As demonstrated by Jaeger et al. [13], the gap between the array and the Kevlar membrane provides significant attenuation of flow-induced noise caused by the unsteadiness of the boundary layer. In the semi-anechoic configuration (Fig. 7b), the 63-element phased array was installed in the anechoic chamber at three locations, labeled from 1 to 3.

The array in position 1 was intended to reproduce the measurement conditions in the hard-walled test section. In this position, the array was also in the near field, straight under the gear, and was recessed 2.75 in. behind the Kevlar window. Comparing results between the near-field streamwise position in this test entry (array position 1) and the entry in the hard-walled test section allows the effects of the acoustic environment on phased-array measurements to be investigated. The relevance of the comparison is emphasized by the fact that both experiments took place in the same facility at the same flow speeds, using the same landing-gear model and the same phased array.

The array in position 2 was located 82.5 in. from the Kevlar wall. The distance d between the array and the model was sufficiently large for the array to be in the acoustic far field ($d > 10\lambda$) and nearly in the geometric far field (d was about three times the largest dimension of the landing gear). Phased-array measurements carried out from this far-field position were compared with the near-field data (position 1). Therefore, the validity of collecting acoustic data with the phased array near the model could be evaluated.

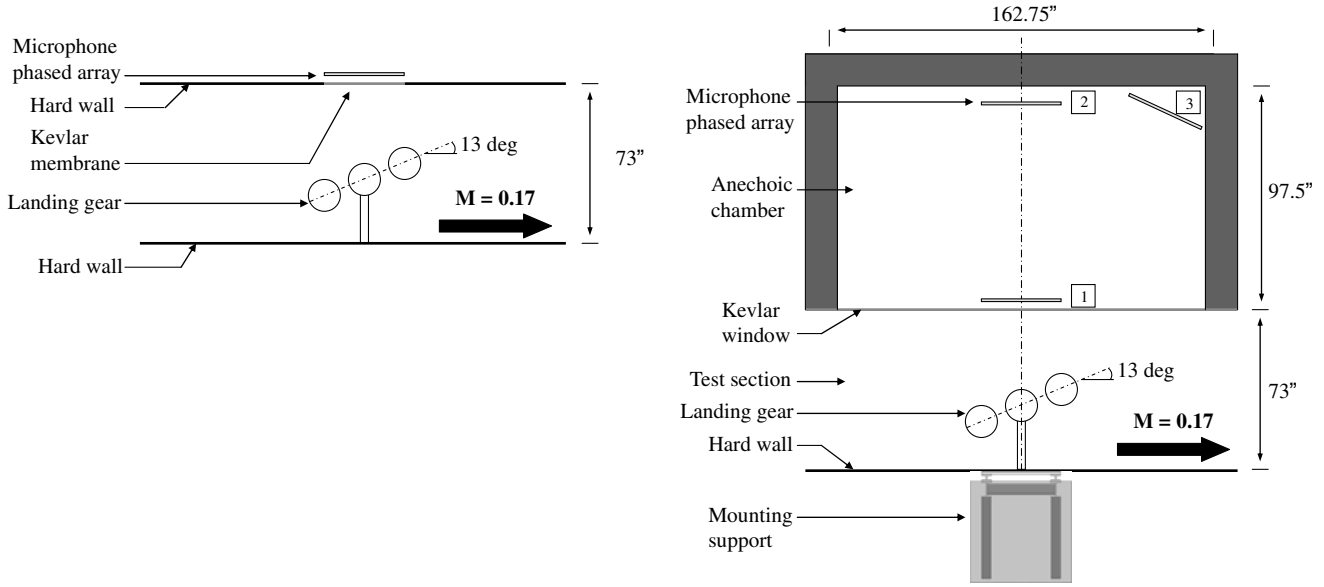

a) b)

Fig. 7 Test setup for phased-array measurements of the landing-gear noise in a) hard-walled and b) semi-anechoic test sections.

Additional far-field measurements were carried out with the array in position 3 (i.e., in the rear arc). The center of the array was located 82.5 in. from the Kevlar wall. To avoid distortion effects, the phased array was oriented such that the normal to its surface was pointing toward the center of the hard-wall window. Data from these measurements were used to determine additional landing-gear noise-source components that cannot be seen with the array straight under the gear.

III. Results

Results on landing-gear noise in the VT hard-walled wind tunnel were shown at $M = 0.17$ [6,7], which is near the highest achievable speed of the facility. For comparison purposes, results are shown at the same speed in the present study. All of the frequencies discussed in this section have been scaled to full-scale frequencies by the following relation:

$$f_{\text{full-scale}} = \text{scale factor} \times f_{\text{measured}} \tag{2}$$

where the scale factor is 0.26.

Phased-array data were postprocessed for over 50 frequency bands in one-twelfth-octave bands. It would be very difficult to show beam-forming maps at all frequencies. Instead, beam-forming maps are shown at selected frequencies. To better aid in the visualization of the key components of the gear noise, cross-sectional plots of the originally generated three-dimensional beam-forming maps are presented. The locations of the cross sections are depicted in Fig. 8a.

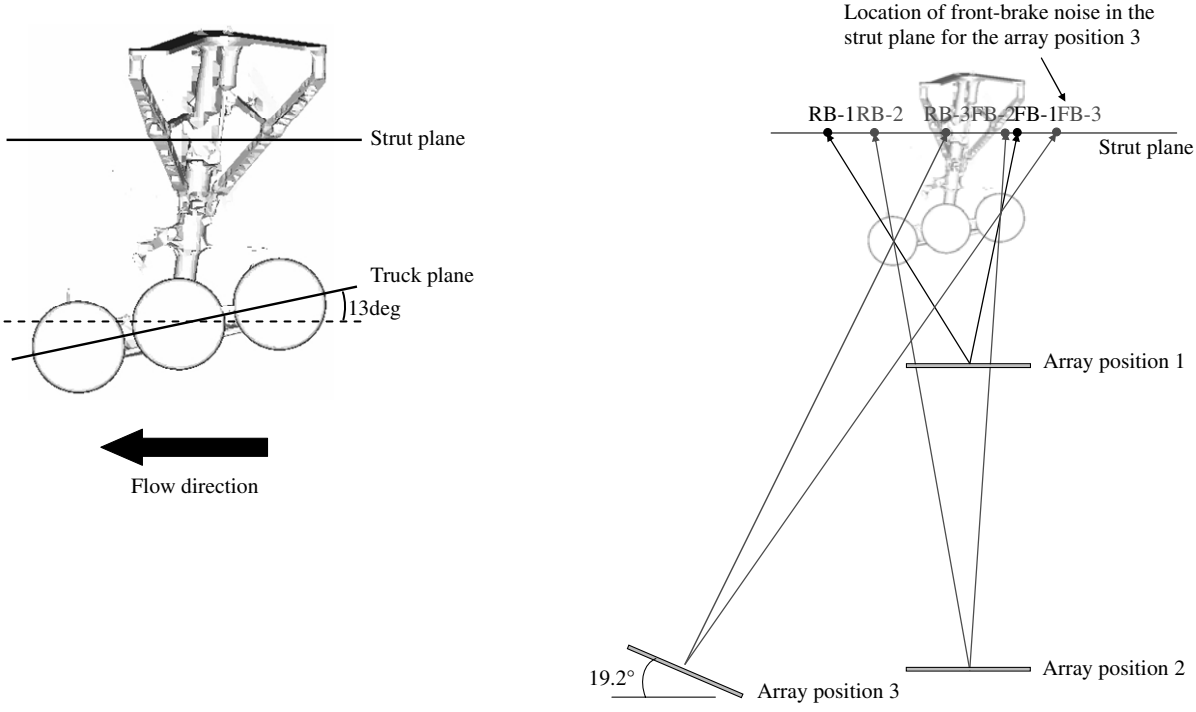

a) b)

Fig. 8 Visualization considerations for the data analysis: a) locations of the strut and truck planes and b) locations of the front- and rear-brake noises projected onto the strut plane for array positions 1 to 3.

The cross sections located at the bottom and at the top are the most representative of the noise generated by the truck and by the strut, door, and braces, respectively. For the sake of clarity, these planes are referred as *truck plane* and *strut plane* in the rest of the paper.

Noise-generated sources on the truck also appear in the strut plane. Depending on the position of the array relative to the gear, the location of the truck noise-source components on the strut plane will vary. This is well illustrated by the schematic shown in Fig. 8b. In this figure and in the rest of the section, FB-*x*, RB-*x*, S-*x*, UB-*x*, and DB-x identify the front brakes, rear brakes, strut, and upstream- and downstream-brace noise sources, respectively, where *x* is an integer between 1 and 3, corresponding to the three array positions

For test entries in both hard-walled and semi-anechoic wind tunnels, the phased array was recessed behind stretched Kevlar. Therefore, the amplitude corrections for the array's output that include the sensitivity of the array, the loss through the Kevlar, and the dissipation effects due to the flow are essentially the same. Although absolute levels of the landing-gear noise were obtained, only relative levels are shown in this paper.

A. Effects of the Acoustic Environment on Phased-Array Measurements

The effects of the acoustic environment on phased-array measurements were investigated by comparison between data collected with the phased array in the near field in hard-walled and semi-anechoic test sections. The discussion is based on the beam-forming maps of the landing-gear noise on the truck plane.

Figure 9 depicts the beam-forming maps of the landing-gear noise with the array in the near field (array position 1 in Fig. 7b), in the hard-walled test section (left), and in the semi-anechoic test section (right). Results for three frequencies are shown in this figure (i.e., full-scale frequencies of 1128, 3381, and 4782 Hz). At each frequency, the reference of 0 dB corresponds to the peak noise value of the beam-forming map obtained in the hard-walled test section.

The figure indicates that in terms of noise-source identification, the beam-forming maps obtained from the tests conducted in hard-walled and semi-anechoic test sections are in good agreement. Indeed, both tests show that for a near-field streamwise position of the array, the front and rear brakes (lower truck components) are the major noise sources of the landing gear. This result is consistent with past noise studies on isolated landing gears with a phased array in the near field of the model [14,15]. The figure also indicates that the reduction of reflections in the test section leads to significantly cleaner beam-forming maps.

In terms of levels, the beam-forming maps indicate that the peak values of the main lobes are higher in the hard-walled test section

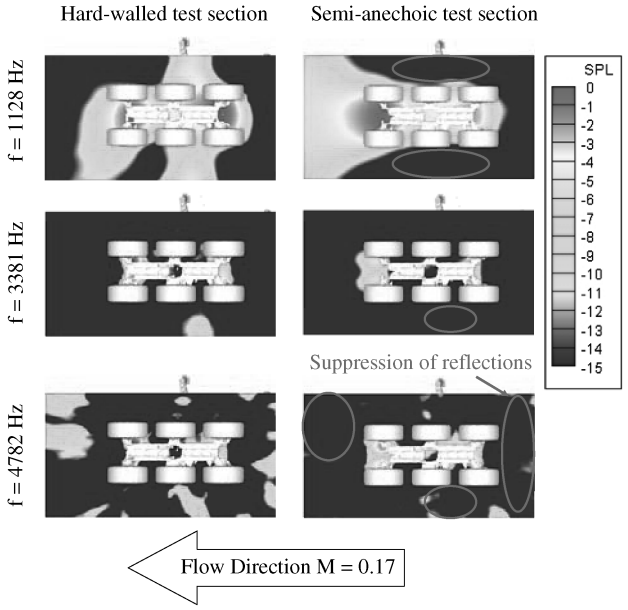

Fig. 9 Beam-forming maps of the landing-gear noise at full-scale frequencies of 1128, 3381, and 4782 Hz, as obtained with the phased array in the near field of the model (position 1).

than in the semi-anechoic test section. A way to quantify this difference in levels is to look at the integrated spectra of the landing-gear noise in hard-walled and semi-anechoic test sections. Integrated spectra are obtained by adding the levels on the maps and normalizing such levels by the point spread function of the array over the desired region. Also, a threshold of 8 dB from the peak value was used to reduce the influence of side lobes on the integration output.

Figure 10a depicts the integrated spectra of the landing-gear noise as obtained in the near field in hard-walled (solid curve) and semi-anechoic (dashed curve) wind tunnels. The curves have similar trends and differ only by a few decibels. This result is remarkable, considering the time elapsed between the two series of tests (about a year and a half) and the modifications conducted on the facility. For better visualization, the difference between the integrated spectra of the landing-gear noise in hard-walled and semi-anechoic test sections is depicted in Fig. 10b. In the figure, a positive value of the curve indicates that the sound pressure level of landing gear is higher in the hard-walled test section than in the semi-anechoic test section. The integrated spectrum of the landing gear in the hard-walled test

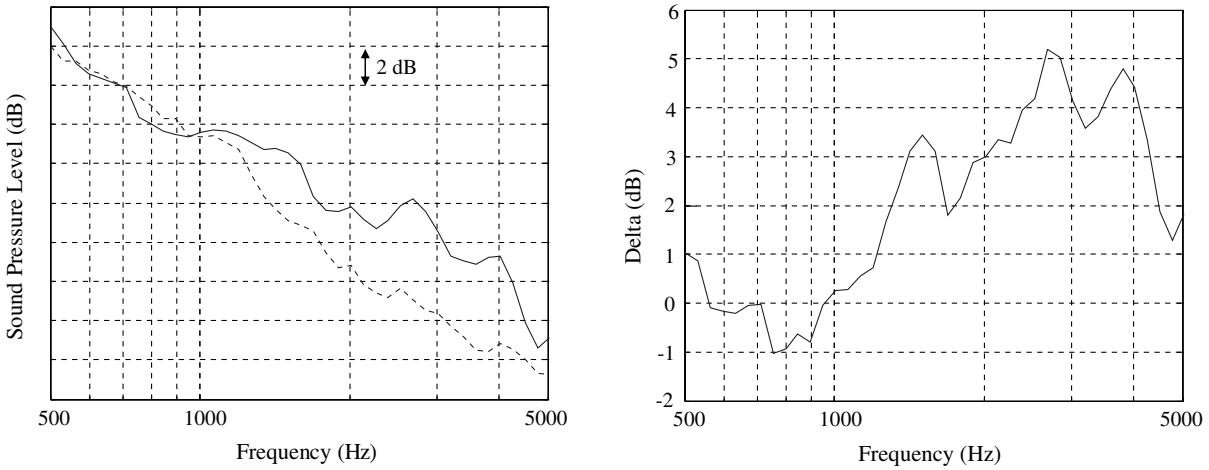

Fig. 10 Comparison between landing-gear noise levels measured in the near field, in the hard-walled and semi-anechoic test sections, as a function of frequency: a) integrated spectra obtained in hard-walled (solid curve) and semi-anechoic (dashed curve) test sections and b) spectral difference.

section is up to 5.2 dB higher than in the semi-anechoic test section. Note that when beam-forming maps are integrated to estimate the sound pressure level of the sources, so are the reflections, which are not representative of the actual noise generated. In other words, the presence of reflections in the beam-forming maps may lead to an overestimation of the actual noise levels generated by the model. Tests were conducted in the same facility at the same speeds, using the same landing-gear model and phased array. Therefore, the difference in levels between hard-walled and semi-anechoic test sections is most likely caused by the presence of reflections in the beam-forming maps obtained in the hard-walled test section.

B. Near-Field Effects on Phased-Array Measurements

The effects of taking aeroacoustic measurements in the near field were investigated by comparison between data collected with the phased array in the near field (position 1) and far field (position 2) in the semi-anechoic test section. Note that moving the array to a different position modifies the resolution of the array over the desired grid. However, in this paper, the beam-forming maps are not used to quantify the levels, but only for noise-source location. The effect of moving the array further away from the model was taken into account when integrating the beam-forming maps by normalizing with the corresponding point spread function.

Figures 11 and 12 depict the beam-forming maps of the landing-gear noise as obtained with the array in the anechoic chamber in positions 1 (left) and 2 (right). Results for full-scale frequencies of 1128, 3381, and 4782 Hz are shown.

First, let us consider the beam-forming maps obtained with the array in the near field (array position 1). For the three frequencies shown, looking at the truck and strut planes indicates that the front and rear brakes are the only noise sources identified. Then the array was moved to the far-field in position 2, which corresponds to the maps on the right in Figs. 11 and 12. As can be seen, the front and rear brakes are still the major noise sources. However, other noise sources may be identified with the array in the far field, such as the noise radiated from the upstream and downstream braces. Noise from the upstream and downstream braces clearly appears on the maps up to 3381 Hz. At 4782 Hz, noise from the upstream brace is no longer identified. Note again that moving the array to a different position modifies the resolution of the array over the desired grid.

The beam-forming maps obtained with the array in the near field and far field were integrated to quantify the contribution from the components hidden by the truck when the array is in the near field. For comparison purposes, the phased-array data collected in the near field (array position 1) were extrapolated to the far field (array position 2) using the spherical spreading law. The integrated spectra of the landing-gear noise in the semi-anechoic test section with the phased array in the near field and far field are shown in Fig. 13a. For ease of comparison, the difference in levels between the far field and extrapolated near-field configurations is plotted in Fig. 13b. In this figure, a positive value means that levels of the landing-gear noise are higher when they are obtained with the array in the far field. The figure shows that the integrated spectra difference reaches maximum values of about 5.3 dB between 1800 and 3300 Hz. At frequencies lower and higher than that range, the integrated spectra difference rolls off from the maximum of around 5.3 to about 1 dB. This result is in very good agreement with the beam-forming maps depicted in Figs. 11 and 12. As mentioned earlier, with the array in the near field, the noise from the braces cannot be identified. However, with the array in the far field, the noise contribution from both braces can be clearly observed up to a frequency of 3381 Hz. At higher frequencies (e.g., 4782 Hz), the contribution from the upstream brace is no longer visible, which explains why the curve in Fig. 13b rolls off between 3300 and 5000 Hz. At frequencies larger than 5000 Hz, none of the braces can be identified as a significant noise source. As a result, the integrated spectra difference between far-field and near-field measurements is only about 1 dB at 5000 Hz.

Both the beam-forming maps and integrated spectra indicate that the brakes are not the only components of the landing-gear noise on the flyover path. As the phased array is moved from the near field to the far-field straight under the gear, the braces appear as major noise-source components. It is suspected that when the array is too close to the landing gear, the truck acts like an acoustic barrier and the components located behind the truck cannot be seen by the array. Also, the integrated spectra suggested that landing-gear noise levels obtained with the array in the near field straight under the gear are underestimated by up to about 5.3 dB between 1800 and 3300 Hz. In other words, the contribution from the braces is the most significant in the frequency range 1800–3300 Hz. These results demonstrate that

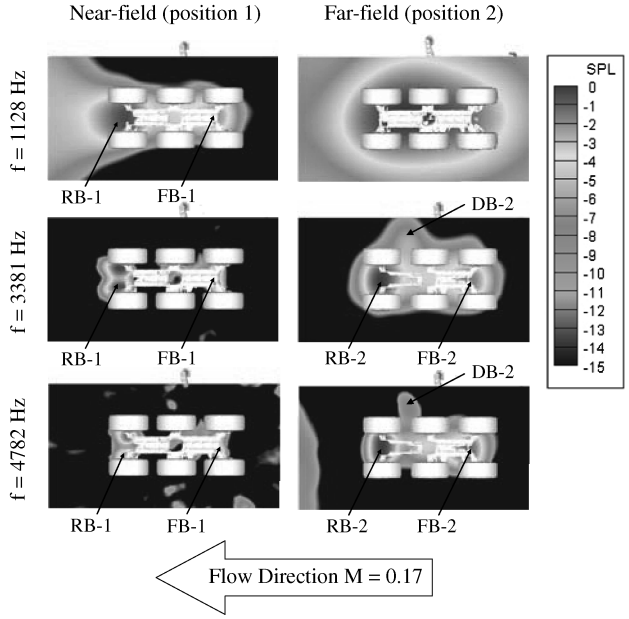

Fig. 11 Beam-forming maps in the truck plane at full-scale frequencies of 1128, 3381, and 4782 Hz, as obtained with the phased array in positions 1 and 2.

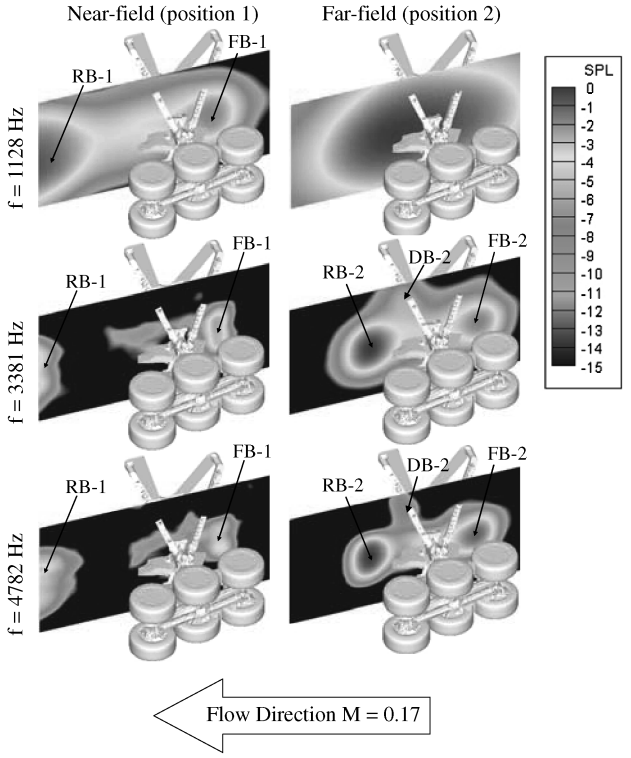

Fig. 12 Beam-forming in the strut plane at full-scale frequencies of 1128, 3381, and 4782 Hz, as obtained with the phased array in positions 1 and 2.

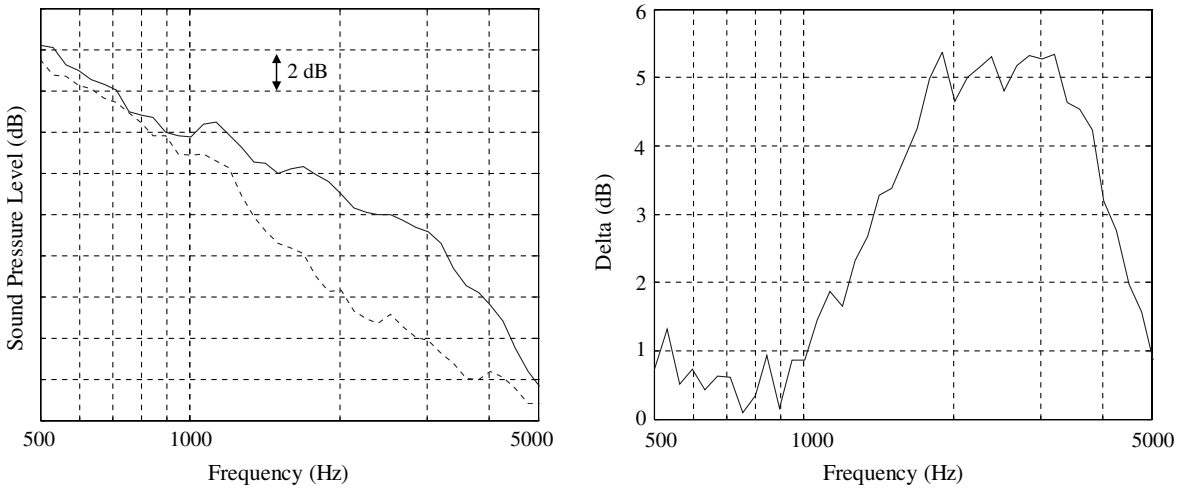

Fig. 13 Comparison between landing-gear noise levels measured in the semi-anechoic test section, in the near and far fields, as a function of frequency: a) integrated spectra obtained in the far field (solid curve) in near field (dashed curve) and b) spectral difference.

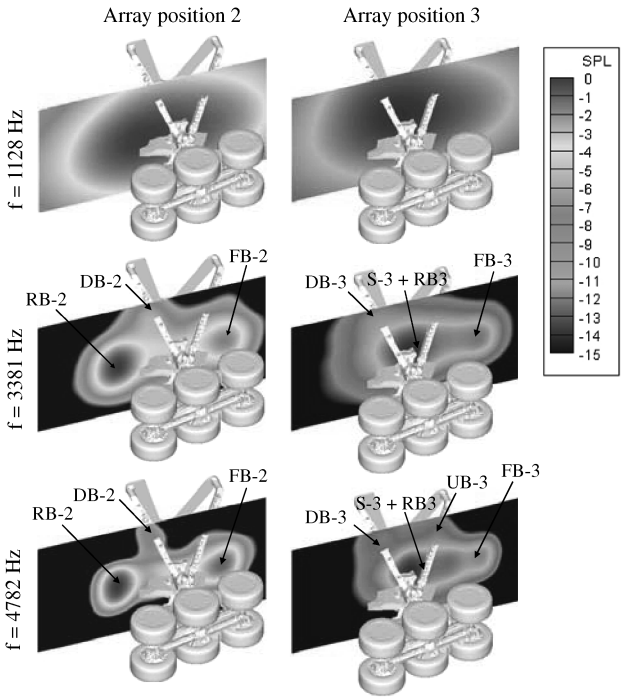

Fig. 14 Beam-forming maps of the landing-gear noise, at full-scale frequencies of 3381 and 4782 Hz, as obtained with the phased array in the anechoic chamber in positions 2 and 3; peak value at each frequency is used as reference (i.e., 0 dB).

streamwise phased-array measurements of the landing-gear noise are not reliable when they are carried out in the near field.

C. Comparison Between Two Far-Field Streamwise Array Positions

It is also very interesting to compare results from different far-field streamwise array positions. Figure 14 shows the beam-forming maps of the landing-gear noise as obtained with the array straight under the gear (maps on the left, array position 2) and in the rear arc (maps on the right, array position 3). Results for full-scale frequencies of 1128, 3381, and 4782 Hz are shown from top to bottom.

As can be seen, the beam-forming maps obtained from array positions 2 and 3 look very different, though both positions are in the far field. As mentioned earlier, when the array is in position 2 (maps on the left), not only can noise from the brakes be identified, but so can noise from the braces. However, the projection of the lower truck noise components on the strut plane (RB-2 and FB-2) indicates that the brakes are still dominant noise sources. For the array in position 3 (maps on the right), a combination of the strut and the rear brake appears as the major noise source. Because of the position of the array relative to the landing gear (Fig. 8b), it is difficult to distinguish these two noise sources from each other.

In terms of levels, significant differences between the results obtained with the array in positions 2 and 3 are observed. For comparison purposes, the phased-array data collected with the array in position 3 were extrapolated so that the distance from the center of the truck to the center of the array was the same for both array positions. The integrated spectra of the landing gear obtained with the array in positions 2 and 3 are shown in Fig. 15a. The integrated spectral difference is shown in Fig. 15b. This figure indicates that over the entire frequency range studied, levels of the landing-gear noise in the rear arc (array position 3) are significantly higher than those straight under the gear (array position 2). The difference in levels is particularly large in the frequency range from 600 to 1500 Hz and reaches a maximum of 4.8 dB at 750 Hz. This difference is most likely caused by the noise contribution of the landing-gear components (such as the strut, the hydraulic cylinder, the lock links, and so forth) that are shielded by the truck when the array is straight under the gear (array position 2).

IV. Conclusions

In this study, it was shown that conducting aeroacoustic studies in hard-wall wind tunnels involves several limitations. Although diagonal removal was used in the postprocessing of the phased-array data to minimize the effects of reflections, beam-forming maps obtained in the hard-walled wind tunnel included more side lobes than those obtained in the semi-anechoic wind tunnel, due to the significantly reverberant conditions. The integration of these spurious sources, which are not related to actual sources on the model, results in an overestimation of the actual noise levels. Also, in hard-walled wind tunnels, the phased array is usually in the near field of the model. In the case of a very complex structure such as the landing gear, some of the noise sources cannot be identified because of shielding effects. Testing in a hard-wall wind tunnel renders difficult the study of the directivity of the sound radiated by a model, because the phased array is usually mounted straight in front of the model. The inability to position the phased-array instrumentation at different radiation locations is detrimental. In the case of the

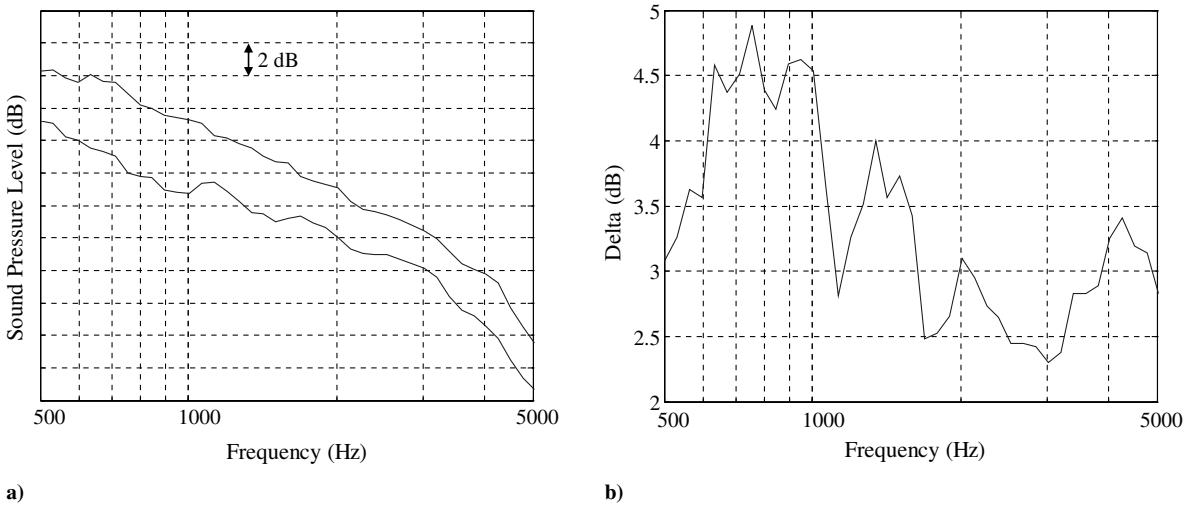

Fig. 15 Comparison between landing-gear noise levels measured in the semi-anechoic test section, in the far field straight under the gear and in the rear arc of the gear, as a function of frequency: a) integrated spectra obtained straight under the gear (solid curve) and in the rear arc of the gear (dashed curve) and b) spectral difference.

landing-gear noise, it was shown that noise measurements directly underneath the landing gear are not the most representative because they will underestimate the radiation. These tests on a model-scale landing gear also allowed for a new wind-tunnel design concept to be validated.

Acknowledgments

The authors would like to acknowledge the financial support from NASA Langley Research Center and its technical monitors Bart Singer and Mehdi Khorrami. The landing-gear model used in this project was also provided by NASA. This financial support is greatly appreciated.

References

[1] Michel, U., Barsikow, B., Helbig, J., Hellmig, M., and Schuettpelz, M., "Flyover Noise Measurements on Landing Aircraft with a Microphone Array," 4th AIAA/CEAS Aeroacoustics Conference, Toulouse, France, AIAA Paper 1998-2336, June 1998.

[2] Lazos, B., "Surface Topology on the Wheels of a Generic Four-Wheel Landing Gear," *AIAA Journal*, Vol. 40, No. 12, 2002, pp. 2402–2411.

[3] Dobrzynski, W., and Buchholz, H., "full-Scale Noise Testing on Airbus Landing Gears in the German Dutch Wind Tunnel," 3rd AIAA/CEAS Aeroacoustics Conference, Atlanta, GA, AIAA Paper 1997-1597, May 1997.

[4] Morse, P. M., and Ingard, K. U., *Theoretical Acoustics*, Princeton Univ. Press, Princeton, NJ, 1968, pp. 761–763.

[5] Guo, Y. P., Yamamoto, K. J., and Stoker, R. W., "Experimental Study on Aircraft Landing Gear Noise," *Journal of Aircraft*, Vol. 43, No. 2, 2006, pp. 306–317. doi:10.2514/1.11085

[6] Ravetta, P. A., Burdisso, R. A., and Ng, W. F., "Wind Tunnel Aeroacoustic Measurements of a 26%-scale 777 Main Landing Gear Model," 10th AIAA/CEAS Aeroacoustics Conference, Manchester, England, U.K., AIAA Paper 2004-2885, May 2004.

[7] Ravetta, P. A., "LORE Approach for Phased Array Measurements and Noise Control of Landing Gears," Ph.D. Dissertation, Dept. of Mechanical Engineering, Virginia Polytechnic Inst. and State Univ., Blacksburg, VA, 2005.

[8] Smith, B. S., Camargo, H. E., Burdisso, R. A., and Devenport, W. J., "Development and Testing of a Novel Acoustic Wind Tunnel Concept," 11th AIAA/CEAS Aeroacoustics Conference, Monterey, CA, AIAA Paper 2005-3053, May 2005.

[9] Crede, E. D., Devenport, W. J., Camargo, H. E., Remillieux, M. C., and Burdisso, R. A., "Calibration and Demonstration of the New Virginia Tech Anechoic Wind Tunnel," 14th AIAA/CEAS Aeroacoustics Conference, Vancouver, Canada, AIAA Paper 2008-2911, May 2008.

[10] Candel, S. M., "Application of Geometrical Techniques to Aeroacoustic Problems," 3rd Aeroacoustics Conference, Palo Alto, CA, AIAA Paper 1976-546, July 1976.

[11] Pierce, A. D., *Acoustics, an Introduction to its Physical Principles and Applications*, Acoustical Society of America, Woodbury, NY, 1989.

[12] Remillieux, M. C., Camargo, H. E., and Burdisso, R. A., "Calibration of a Microphone Phased Array for Amplitude in the Virginia Tech Anechoic Wind Tunnel," NOISE-CON 2007, Inst. of Noise Control Engineering Paper NC07-335, Oct. 2007.

[13] Jaeger, S. M., Horne, W. C., and Allen, C. S., "Effect of Surface Treatment on Array Microphone Self-Noise," 6th AIAA/CEAS Aeroacoustics Conference, Lahaina, HI, AIAA Paper 2000-1937, June 2000.

[14] Jaeger, S. M., Burnside, N. J., Soderman, P. T., Horne, W. C., and James, K. D., "Microphone Array Assessment of an Isolated 26%-Scale, High-Fidelity Landing Gear," 8th AIAA/CEAS Aeroacoustics Conference, Breckenridge, CO, AIAA Paper 2002-2410, June 2002.

[15] Smith, M. G., Fenech, B., Chow, L. C., Molin, N., Dobrzynski, W., and Seror, C., "Control of Noise Sources on Aircraft Landing Gear Bogies," 12th AIAA/CEAS Aeroacoustics Conference, Cambridge, MA, AIAA Paper 2006-2626, May 2006.

E. Gutmark
Associate Editor